Appl. Phys. B 33, 205–208 (1984)

Applied Physics B Photophysics and Laser Chemistry

Applications of Two-Photon Absorption for Detection of CO in Combustion Gases

M. Aldén, S. Wallin, and W. Wendt

Department of Physics, Lund Institute of Physics, P.O. Box 725, S-220 07 Lund, Sweden

Received 25 November 1983/Accepted 21 December 1983

Abstract. Laser-induced fluorescence has been used for detection of CO in different environments. The fluorescence light was obtained by using a two-photon transition between the $X^1\Sigma^+$ and the $B^1\Sigma^+$ electronical states around 230 nm. Cell measurements indicate a detection limit lower than 0.1 ppm. Measurements in a CH_4/air flame and in a low pressure dc discharge were realized with a diode-array detector, which was used in an imaging mode, permitting single-shot CO distributions to be captured.

PACS: 33, 82.40

During the last years, laser techniques have gained increasing value in the detection of molecules, radicals and atoms in combustion environments. The most promising techniques so far are; laser-induced fluorescence, Raman scattering and Coherent anti-Stokes Raman Scattering (CARS). The basics of these techniques are covered in several review articles, e.g. [1–3].

The most promising technique for detection of small quantities is laser-induced fluorescence, in which the laser frequency is tuned to an absorption line of a specific specie. By measuring the subsequent reemission of radiation it is possible to infer the concentration of the exciting molecule. From being a technique limited to species absorbing in spectral regions attainable with dye lasers, e.g. CH and C_2, its application was extended to molecules absorbing in the ultraviolet region, down to ~220 nm, by using nonlinear optical mixing techniques. In this way it became possible to detect other molecules of great importance in combustion processes, e.g. OH and NO.

However, there was still a great need for detecting species absorbing in the vuv region, like the atoms O, N, C, and H. The detection possibility for these species (O, N) under well-defined conditions was demonstrated by Bischel et al. [4] in two-photon absorption measurements. Shortly afterwards the first flame measurement of oxygen atoms using two photon absorption was reported [5], followed by flame detection of H [6].

Besides being extended to shorter wavelengths, the laser-induced fluorescence technique has recently been developed for space resolved detection of flame radicals (OH) using optical multichannel detection. First one-dimensional imaging was demonstrated [7], followed by two-dimensional visualization [8, 9] and dual species (OH, C_2) imaging [10].

In the present work we have used two photons at 230 nm to excite the $B^1\Sigma^+ \rightarrow X^1\Sigma^+$ electronical transition in CO for spatially resolved CO measurements in a CH_4/air flame, and in a dc electrical discharge. Prior to these combustion measurements, cell measurements were performed aiming at determination of detection limits, and fundamental constants like lifetimes and quenching cross-sections.

Some experiments were also performed at different CO pressures in order to compare the sensitivity of the fluorescence technique with that of optogalvanic measurements.

In the cell experiments as well as in the combustion experiments it was realized, that under certain circumstances C_2 radicals were created by the focused laser beam. This was also found in our earlier dual-species experiments [10].

CO has previously been investigated using two-photon excitation of the $A^1\Pi \rightarrow X^1\Sigma^+$ transition in cell measurements [11, 12] and in flames [13], whereas the $B^1\Sigma^+ \rightarrow X^1\Sigma^+$ transition recently was investigated in cell measurements by Loge et al. [14], mainly aiming at determining lifetimes and quenching cross-sections.

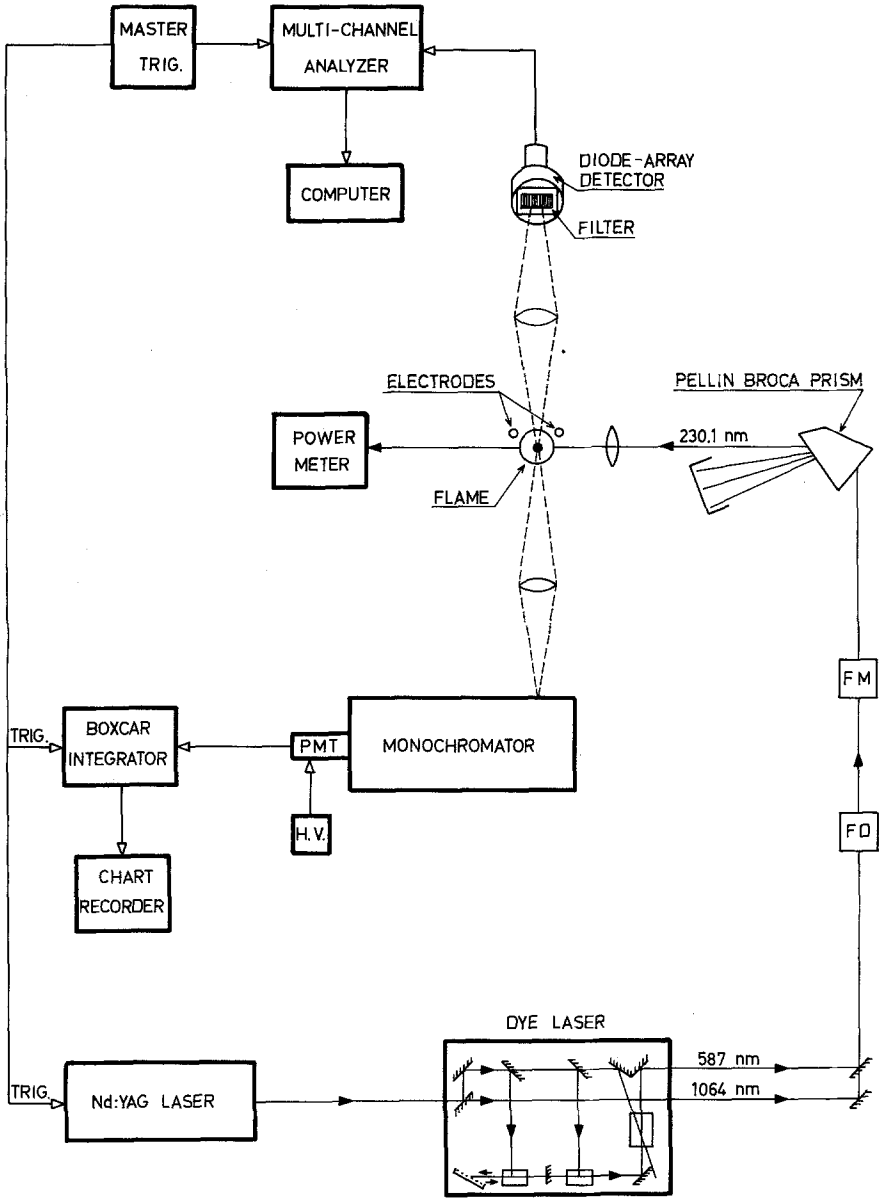

Fig. 1. Experimental set-up used for detection of CO by two-photon absorption

1. Experimental Set-Up

A scheme of the experimental set-up used in the CO experiments is shown in Fig. 1. A Quanta-Ray DCR-1A pulsed Nd:YAG laser with a repetition rate of 10 Hz was used. The pulse length was about 6 ns in the normal Q-switched operation, and the infrared pulse energy was typically 700 mJ. This radiation was frequency doubled to 532 nm and served as the pump source for a Quanta-Ray PDL-1 tunable dye laser. The pulse energy from the dye laser operating with Kiton red as dye was typically 60 mJ at 587 nm. In order to achieve the two-photon excitation wavelength at 230 nm, the dye-laser beam was first frequency doubled to 294 nm, then frequency mixed together with the Nd:YAG fundamental at 1.064 μm. The frequency doubling (FD) and frequency mixing (FM) were made in KD*P crystals. For spectrally separating the laser beam at 230 nm from the infrared, dye and doubled-dye beams a Pellin-Broca quartz prism was used. The beam was then focused into the flame with a $f = 500$ mm quartz lens. The long focal length was chosen because it provides a more uniform beam-waist through the flame. The pulse energy at 230 nm, which was measured behind the flame, was typically 2 mJ. It was found that the pulse energy was critically dependent on the number of reflections in quartz prisms and mirrors. Directly after the Pellin-Broca prism the pulse energy exceeded 4 mJ.

In the cell measurements, a cell equipped with quartz windows mounted at Brewster's angel was used. The optogalvanic signals could be registrated simultaneously with the fluorescence light by means of two metallic plates mounted in the cell, 10 mm apart. The signal was viewed on a Tektronix 475 oscilloscope. The voltage between the plates was typically 1000 V. The burner used in the flame experiment was made in such a way so that the premixed CH_4/air gases were led through a 300 mm water-cooled tube, to assure a laminar gas flow. The fluorescence light was detected at right angels in two different arrangements. In one approach the fluorescence light was detected with a diode-array detector, whereas in the other arrangement a photomultiplier tube was used. The detector array, a Tracor Northern TN-1223-4IG unit with an image intensifier, and gatable down to 0.3 μs, was connected to a Tracor Northern TN-1710 main frame. The diode-array detector, consisting of 1024 diodes, 25 μm × 2.5 mm each, was placed in the image plane of an UFS 200 Jobin Yvon spectrograph for capturing spectra covering the 200–800 nm spectral region. Alternatively, it was used for imaging experiments. In these experiments the laser beam-waist was imaged on to the detector array with a $f = 100$ mm lens. In front of the detector a Schott GG 475 coloured glass filter and a Corion 580 nm cut on filter, were used to isolate the laser induced fluorescence originating from the CO molecules. In both the imaging and spectral mode the light intensities were digitized in the Tracor system and were stored on floppy discettes in a PDP-11/*VO* 3 mini computer system for subsequent data processing.

In the experiments using photomultiplier detection, the fluorescence light was collected with a lens matching a $f/4.4$ Bausch & Lomb monochromator with a dispersion of 0.8 nm/mm. As detector an EMI 9816 JQB photomultiplier tube with a risetime of 2.2 ns was used. A PARC Model 162 boxcar integrator, equipped with two Model 165 gated integrators, was then used to process the signals, which after averaging yielded the output signal for a chart recorder. The photomultiplier detection approach was used in the lifetime measurements and for the detection of small amounts of CO.

2. Measurements and Results

As was indicated in the introduction the measurements consisted of two different parts. In one part measurements were made in a cell and in the other one experiments were performed in a flame and in an electrical discharge.

In all experiments the CO molecules were excited from their ground state, $X\,^1\Sigma^+$ to the $B\,^1\Sigma^+$ state using two photons at 230 nm. These transitions belong to the so called Hopfield-Birge systems of the CO molecule.

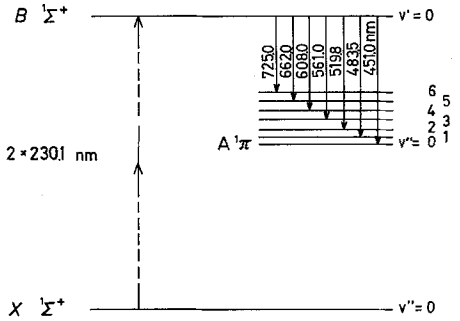

Fig. 2. A schematic energy-level diagram showing the two-photon absorption and fluorescence wavelengths

After a short time, part of the excited molecules are radiatively transferred to vibrational levels of the $A\,^1\Pi$ state with light emission between 451 and 725 nm. By detecting this laser induced fluorescence, belonging to the so called Ångström system, the presence of CO could be acertained. A schematic energy-level diagram of the two-photon absorption and consequent fluorescence wavelengths is shown in Fig. 2.

2.1. Cell-Measurements

Although the original aim for the experiments described in this paper was to use the two-photon absorption technique for spatially resolved measurements in flames and discharges, the first experiments were performed with CO in a cell. The fluorescence spectrum of the $B\,^1\Sigma^+ \rightarrow A\,^1\Pi$ transitions following the absorption of two photons at 230 nm is shown in Fig. 3. This spectrum was recorded using the diode-array detector at the exit plane of the Jobin Yvon spectrograph. As can be seen, it was possible to observe the fluorescence light originating from $B\,^1\Sigma^+$ ($v'=0$) to $A\,^1\Pi$ ($v''=0, 1 \ldots 6$). The spectrum shown was obtained with 10 Torr of CO in the cell. By tuning the dye laser wavelength off CO resonance it was checked that the fluorescence light really orginated from CO molecules. In addition to the $B\,^1\Sigma^+ \rightarrow A\,^1\Pi$ band, transitions due to the $b\,^3\Sigma^+ \rightarrow a\,^3\Pi$ band could be seen between 300 and 350 nm. These transitions arise because the $b\,^3\Sigma^+$ and the $B\,^1\Sigma^+$ states are energetically close-lying, $T_e = 83814$ and 86945 cm^{-1}, respectively [15]. Thus, the $b\,^3\Sigma^+$ state is populated through collisions.

As was shown by Moore and Robinson [16] in lifetime measurements of the $B\,^1\Sigma^+$ ($v'=0$) state using the phase-shift method, the effective lifetime depends on the CO pressure. This is due to the large Franck-Condon factor of the $B\,^1\Sigma^+$ ($v'=0$) $\rightarrow X\,^1\Sigma^+$ ($v''=0$) transition, which leads to resonance trapping of the corresponding radiation. The Franck-Condon factor for the (0, 0) transition has been calculated to be 0.988 [16, 17]. It has also been shown that in the limit of low

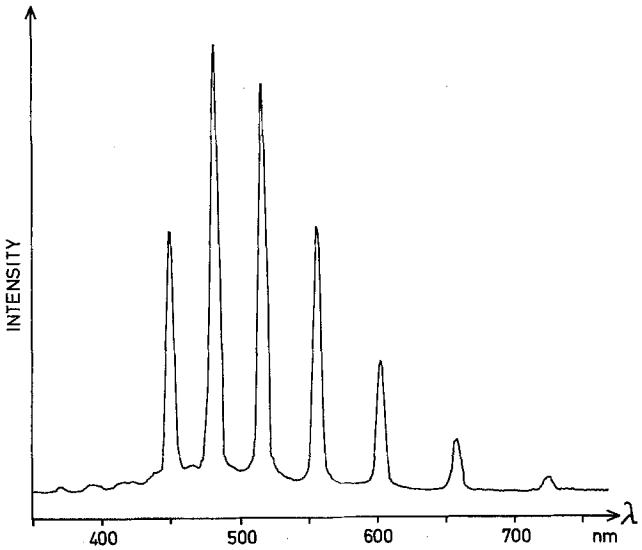

Fig. 3. Laser-induced fluorescence spectrum of CO

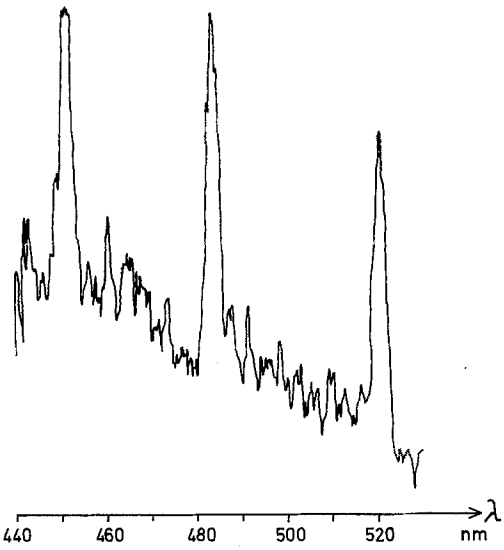

Fig. 4. Laser-induced fluorescence spectrum from ~0.2 ppm CO

CO pressure (~5 mTorr) the inherent lifetime of the $B^1\Sigma^+$ state is 22 ns, whereas in the case of total trapping the lifetime is increased by a factor of ~2.7 [17].

We have measured the effective lifetime of the $B^1\Sigma^+$ state in the high-pressure regime by detecting the fluorescence in the (0, 1) band at 483.5 nm. The decay rates were measured between 1 and 5 Torr using the PARC Boxcar integrator with a scanning time window of 5 ns. A Stern-Volmer plot yielded a straight line where the intercept gave the lifetime, whereas the self-quenching rate was inferred from the slope. The results from our preliminary experiments were for the lifetime; 60 ns and for the CO self-quenching rate; 7.8 $\times 10^6$/Torr s, which is in fairly good agreement with recently reported measurements of 68 ns and 5.9 $\times 10^6$/Torr s [14].

During the cell measurements it was observed that the fluorescence light was extremely strong. Above 10 Torr of CO in the cell, the fluorescence light clearly appeared as a blue-green streak, and at even higher CO pressures part of the scattered light appeared as superfluorescence collinearly with the incident 230 nm laser beam. Very recently two-photon pumping of CO has been used for obtaining laser action at 484 and 520 nm [18]. In order to test the two-photon absorbtion technique for detection of small CO contents in combustion gases, 1 Torr of CO was diluted in 500 Torr of air, which was pumped down to 1 Torr with subsequent dilution in air. Proceeding in this way it was found possible to detect sub ppm levels of CO. A spectrum of ~0.2 ppm CO is shown in Fig. 4. In this experiment one cut-off and one cut-on filter was used to surpress scattered laser light below 430 and above 540 nm. The time constant on the Boxcar integrator was 8 s. As can be seen the (0, 0), (0, 1), and (0, 2) bands are superimposed on a red degraded background, which is due to laser induced fluorescence in cell windows and walls. This experimental set-up which was not pushed to its limit what regards low CO detectivity, could easily be optimized at least a factor of ten by increasing the solid angle, by using a multiple pass arrangement and by lowering the background fluorescence.

In a previous CO study Sullivan and Crosley [13] used two photons at 290 nm to excite the $A^1\Pi \rightarrow X^1\Sigma^+$ band and by detecting at 197 nm in the same electronical band, the detection limit was set to 0.5% mol fraction.

In order to compare the fluorescence and optogalvanic detection techniques, corresponding signals were recorded for CO pressures varying from 1–20 Torr in N_2 with a total pressure of 110 Torr. As before, the fluorescence signal was obtained by comparing the ratio on/off CO resonance. The optogalvanic signal was obtained simultaneously as the fluorescence signal on an oscilloscope. By varying the voltage across the plates, it was found that with our probe the optimal voltage was 1000 V. Below 5 Torr of CO the optogalvanic approach gave a higher on/off ratio, whereas above 5 Torr the fluorescence technique was clearly advantageous.

When using more than ~25 Torr of CO in the cell, it was clearly evident that additional peaks appeared in the fluorescence spectrum. These peaks, that were found to originate from C_2 radicals, (the so-called Swan bands), were very obvious at larger CO pressure and were more laser-power dependent than the corre-

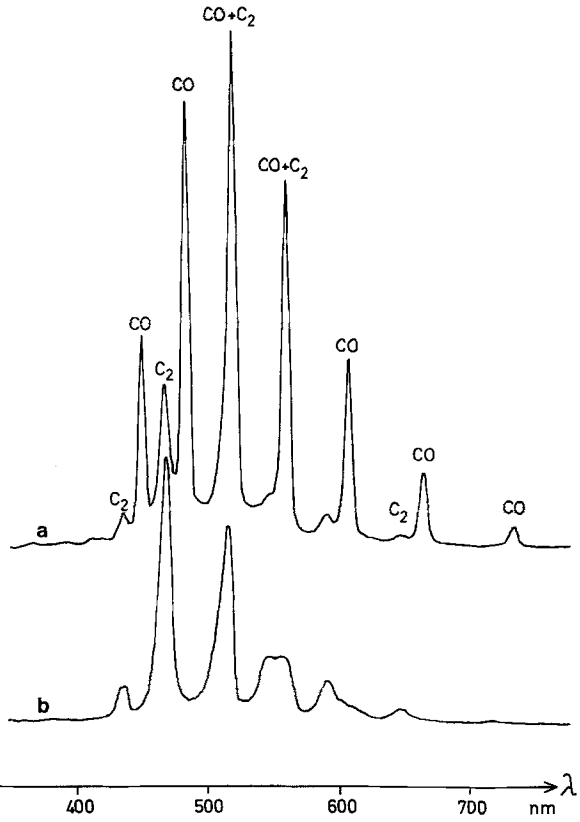

Fig. 5. (a) Laser-induced fluorescence spectrum of CO and the emission from created C_2 radicals when gating the detector array directly on the laser pulse. (b) Emission from created C_2 radicals when the gating of the detector array is delayed $\sim 3\,\mu s$

sponding CO signals. By varying the 0.3 μs gate on the diode-array detector it was evident that the C_2 emission extended for a much longer time period than the almost prompt (at this pressure) CO emission. This is shown in Fig. 5 where Fig. 5a shows the spectrum of the CO and C_2 bands at a pressure of 300 Torr of CO in the cell and gating directly on the laser pulse. The spectrum in Fig. 5b was recorded in the same way, the only difference is that the gate is now delayed $\sim 3\,\mu s$. During these experiments it was realized that tuning the laser wavelength off CO resonance did not only cause the CO fluorescence to disappear, also the C_2 emission intensity was decreased by about a factor of twenty.

The C_2 Swan emission has previously been studied by multiphoton uv excitation of CO off resonance at 266 nm [19].

In the above described cell measurements lenses with different focal length were also used. When using a $f = 50$ mm lens it was shown that an increase of laser energy by 40% around 1 mJ only increased the signal strength by 20%, which is far from the quadratic dependence on the laser intensity which would be

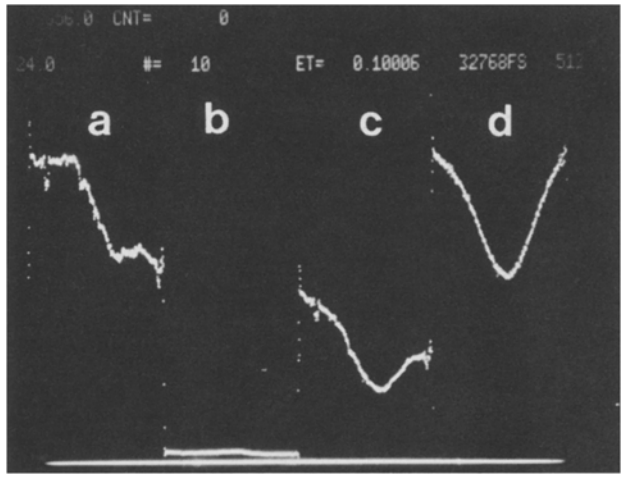

Fig. 6. (a) Scattered CO fluorescence distribution, as shown on the Tracor CRT without any discharge and a pressure of 75 Torr in the cell. (b) Background distribution when tuning the laser wavelength off CO resonance. (c) Scattered light distribution when the dc discharge is on in the cell. (d) Curve (c) divided by curve (a), when corrected for background

expected for a pure two-photon process. Thus, it seems that in addition to the above described photoionization process, a considerable degree of saturation is reached.

2.2. *Combustion Measurements*

As was described in the introduction a great effort is now put into imaging experiments and flow visualization in several laboratories. In this paper we report on imaging experiments in a dc discharge and in different flames.

In order to describe how the spatial distributions of CO were obtained, the dc discharge experiments may serve as an example. CO at a pressure of 75 Torr was kept in a cell made of plexiglass with fused quartz windows for transmitting the laser beam and for detecting the fluorescence. The electrodes, made of stainless steel, were fed with 6 kV, 6 mA and were kept 60 mm apart, which produced a stable dc discharge. In Fig. 6a it is shown how the spatial distribution appeared on the Tracor Northern CRT without any discharge and the laser tuned to the CO resonance. As can be seen, the distribution is far from straight and smooth, which is the result of a non-uniform response across the diode array and the intensity distribution of the laser beam. Figure 6b shows the distribution when the laser frequency is tuned off resonance, which shows, that the signal in Fig. 6a is due to CO molecules. The fluorescence light when the discharge is on, and the laser is tuned to the resonance is shown in Fig. 6c. The resulting CO distribution in the discharge when

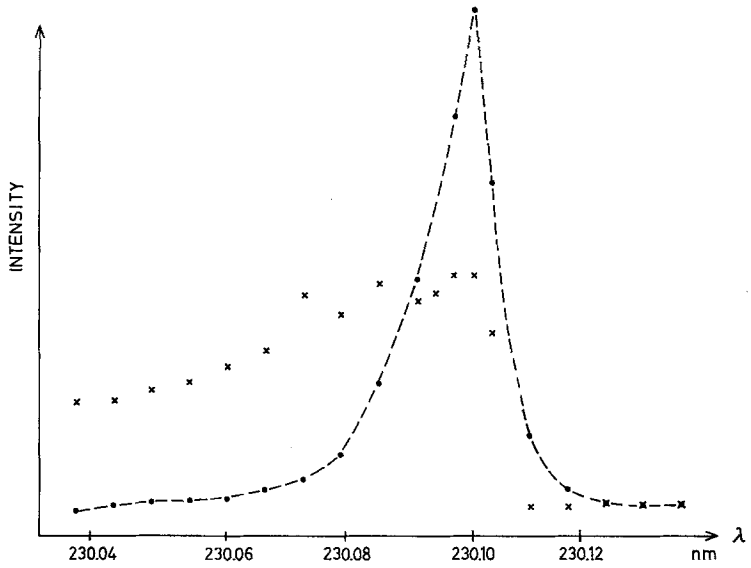

Fig. 7. Excitation spectrum of CO molecules in a cell ●. Excitation spectrum of CO in a CH_4/air flame (×). As a guidence for the eye the cell spectrum is indicated by a broken line

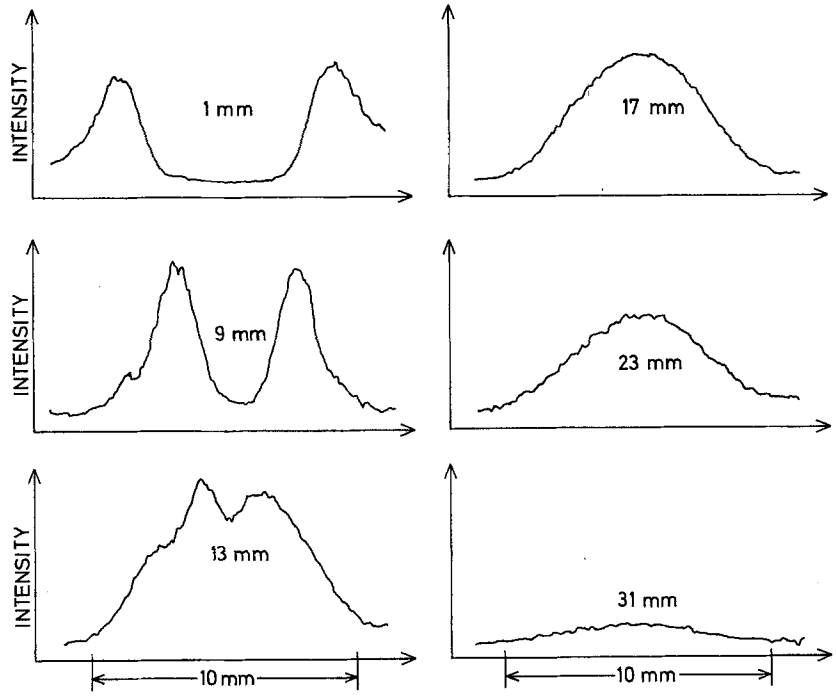

Fig. 8. The spatial distributions of scattered light intensities from CO molecules at different heights above the burner in a CH_4/air flame

corrected for the nonuniform response and the background is shown in Fig. 6d. As can be seen, the distribution is symmetric and the discharge channel is clearly shown. The distributions in Fig. 6a–c are in scale whereas the one in Fig. 6d is multiplied by a constant factor since division of the distributions in Fig. 6a and c was performed with a Tracor Northern Photometric Processor Module TN-1710-29 and required a multiplication factor to yield high resolution. The ratio between a) and c) as shown in d) range from 55% down to 35% in the center of the discharge channel. In Fig. 6 all distributions correspond to a covered distance of 12 mm in the discharge cell.

Flame experiments were performed in several different flames, e.g. CH_4/air, C_3H_8/air, and CO/air. The excitation spectrum of CO at the top of a CH_4/air flame is shown in Fig. 7. In this spectrum the fluorescence light was detected in the (0, 1) band at 483 nm, while scanning the wavelength of the dye laser. No automatic tracking devices were available for the doubling and

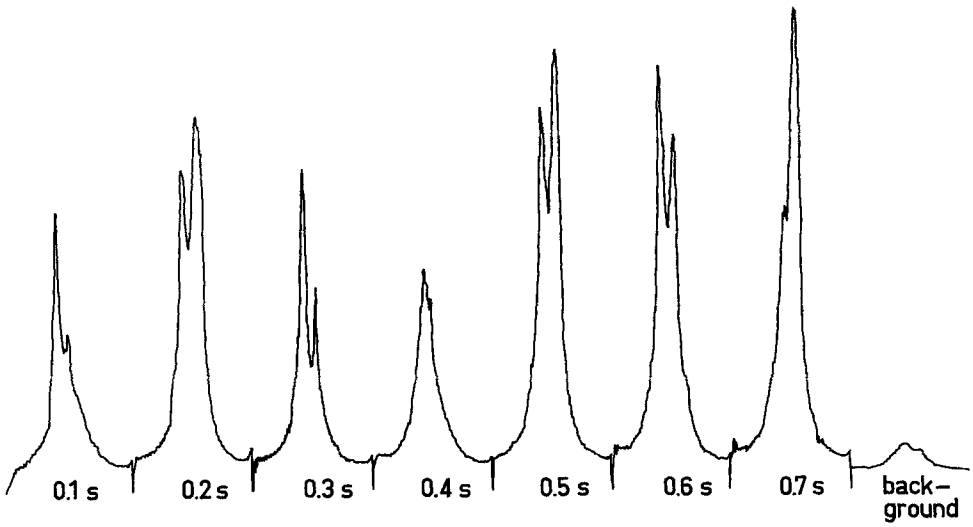

Fig. 9. Seven sequential single shot fluorescence distributions at the top of a turbulent C_3H_8/air flame. To the right is shown the light distribution when tuning the laser wavelength off CO resonance

mixing crystals for fulfilling the phase-matching conditions while changing the wavelength of the dye laser. Therefore the spectrum was recorded by optimizing the laser energy for each wavelength setting. This approach is clearly not adequate for a detailed spectrum. However, it is evident that the flame spectrum is much broader than the one from the cell, which is also shown for comparison. Shown in Fig. 7 is the Q-branch of the $B^1\Sigma^+(v'=0)\rightarrow X^1\Sigma^+(v''=0)$ transition. The band is degraded towards the blue and the rotational structure is not resolved, since the difference between the rotational constants B in the two states is very small.

In the flame imaging experiments a CH_4/air premixed flame produced on the 300 mm burner was used. The resulting CO distributions at different heights above the burner head in the stable conical flame are shown in Fig. 8. All these distributions are achieved in the same way as described for the discharge experiments. A potential problem in these experiments was the production of C_2 radicals, now in the unburnt fuel, i.e. up to a height of ~ 15 mm. However, this could be avoided by optical filtering of the fluorescence light. The distributions shown in Fig. 8 were obtained by averaging over 20 laser pulses. As can be seen in Fig. 9, single shot registration did not cause any problem. In this figure, seven sequential CO distributions were registrated using the Tracor Northern Sequential Scan Module TN-1710-37. The flame used in this experiment was a simple Bunsen burner, fuelled with propane, producing a highly turbulent conical flame. The distributions were recorded at a height of 20 mm above the burner, just at the top of the flame cone. The distributions were recorded at 10 Hz, and for comparison, a distribution captured with the laser tuned off CO resonance, is shown to the right.

3. Conclusion

We have demonstrated in this paper that the two-photon absorption technique is well suited for detection of CO both in exhaust gases and in flames. In combination with diode-array detection, the capturing of single pulse spatially resolved flame distributions is quite feasible. A potential problem, here as well as was pointed out in [10], is the production of C_2 radicals. In that study it was possible to control the degree of C_2 created by the laser beam, by tuning the laser wavelength off OH resonance, and thereby separating the OH and C_2 laser caused emissions. However, in this work it was shown that the production of C_2 radicals was sensitive to the laser wavelength. Therefore, great care has to be taken in order to avoid this problem. Previous works [20, 21] have reported the production of C_2 radicals in CARS studies and found that the reason was decomposition of soot particles. We conclude from our work that, in addition to this thermal decomposition, multiphoton uv excitation of CO may contribute to these C_2 signals.

The imaging of CO may be of great importance in ignition experiments, in addition to the well established imaging of OH, which are under way to be applied in this context both in our group as well as in others [22].

Acknowledgements. The authors greatly acknowledge the support of Prof. S. Svanberg. Stimulating discussions with Prof. T. Högberg and Dr. G. Holmstedt are also appreciated. This work was financially supported by the Swedish Board for Technical Developments.

References

1. Laser Probes for Combustion Chemistry, ACS Symposium Series, ed. by D.R. Crosley (American Chemical Society, Washington, DC 1980)
2. A.C. Eckbreth, P.A. Bonczyk, J.F. Verdieck: Prog. Energy Combustion Sci. **5**, 253 (1979)
3. M. Aldén: Applications of Laser Techniques for Combustion Studies, LUTFD2/(TFAF-1005), Ph. D. Thesis, Lund University of Technology, Lund (1983)
4. W.K. Bischel, B.E. Perry, D.R. Crosley: Appl. Opt. **21**, 1419 (1982)
5. M. Aldén, H. Edner, P. Grafström, S. Svanberg: Opt. Commun. **42**, 244 (1982)
6. R.P. Lucht, J.T. Salmon, G.B. King, D.W. Sweeney, N.M. Laurendeau: Opt. Lett. **8**, 365 (1983)
7. M. Aldén, H. Edner, G. Holmstedt, S. Svanberg, T. Högberg: Appl. Opt. **21**, 1236 (1982)
8. M.J. Dyer, D.R. Crosley: Opt. Lett. **7**, 382 (1982)
9. G. Kychakoff, R.D. Howe, R.K. Hanson, J.C. McDaniel: Appl. Opt. **21**, 3225 (1982)
10. M. Aldén, H. Edner, S. Svanberg: Appl. Phys. B **29**, 93 (1982)
11. S.V. Filseth, R. Wallenstein, H. Zacharias: Opt. Commun. **23**, 231 (1977)
12. R.A. Bernheim, C. Kittrell, D.K. Veirs: Chem. Phys. Lett. **51**, 325 (1977)
13. B.J. Sullivan, D.R. Crosley: Bull. Am. Phys. Soc. **27**, 882 (1982)
14. G.W. Loge, J.J. Tiee, F.B. Wampler: J. Chem. Phys. **79**, 196 (1983)
15. K.P. Huber, G. Herzberg: *Molecular Spectra and Molecular Structure IV.* Constants of Diatomic Molecules (Van Nostrand, New York 1979)
16. J.H. Moore, Jr., D.W. Robinson: J. Chem. Phys. **48**, 4870 (1968)
17. F.J. Comes, E.H. Fink: Z. Naturforsch. **28a**, 717 (1973)
18. Laser Focus, p. 22 (Nov. 1983)
19. W.L. Faust, L.S. Goldberg, B.B. Craig, R.G. Weiss: Chem. Phys. Lett. **83**, 265 (1981)
20. A.C. Eckbreth: J. Appl. Phys. **48**, 4473 (1977)
21. D.A. Greenhalgh: Appl. Opt. **22**, 1128 (1983)
22. R. Cattolica: Sandia Lab. Livermore (private communication)